Propagation Characteristics for Dielectric Waveguide Composed of Dielectric Circular Cylinder with Air-hole Cylinder Array

Ryosuke Ozaki, Tsuneki Yamasaki
College of Science and Technology, Nihon University, 1-8-14 Surugadai, Kanda, Chiyoda-ku, Tokyo, Japan

***Abstract* - In this paper, we analyzed the guiding problem for dielectric waveguides composed of dielectric circular cylinder array with air hole cylinder array by the case of shifting the adjacent dielectric of defect regions, and investigated the complex propagation constants at the first stop band region and energy distribution at the guiding mode by using the combination of improved Fourier series expansion method and multilayer method.**

***Index Terms* — waveguide, propagation, guiding problem, dielectric circular cylinders**

1. Introduction

Photonic crystals [1-2] with periodicity into arbitrary direction are very interesting fields in design or fabrication of optics and electronics devices. In general, the photonic crystals are well known as optical nanostructures with periodic of electric permittivity properties. Furthermore, to control the electromagnetic waves or light in the photonic crystal structures formed by circular cylinder array, it is possible to produce the frequency domain which electromagnetic mode cannot exist. Its region is known as photonic band gaps or stop band region [2]. Therefore, it is extremely important to examine its region such as photonic band gap region.

In recent papers [3-4], we have analyzed the guiding problem for dielectric waveguide with defect region in one period composed of dielectric circular cylinder and air-hole cylinders array, and examined the influence for both radius of cylinder and circular cylinder of the middle layer by propagation characteristics analysis for TE mode.

In this paper, we analyzed the guiding problem for dielectric waveguides composed of dielectric circular cylinder array with air hole cylinder array by the case of shifting the adjacent dielectric of defect regions, and investigated the complex propagation constants at the first stop band region and energy distribution at the guiding mode by using the combination of improved Fourier series expansion method and multilayer method.

2. Method of analysis

Let us consider the dielectric waveguide composed of dielectric circular cylinder and air-hole circular cylinder array as shown in Fig.1. The structure of Fig.1 has periodic length p along the z-direction, and is uniform in the y-direction. The regions S_1 and S_3 are defined by dielectric constants ε_0 and permeability μ_0. In the region S_2, the width of each layer and all region are defined by d, $D(=Ld)$, respectively. The middle layer region has only dielectric circular cylinder with cross section area ($b\times c$) and permittivity profile $\varepsilon_3^{(m)}$. And also, dielectric constants are assumed to be ε_a at background medium of the first layer and dielectric circular cylinder in the second layer. The time factor of the electromagnetic fields is $\exp(-i\omega t)$ and will be omitted in the field expression. In the following formulation or analysis, we consider only TE dominant mode.

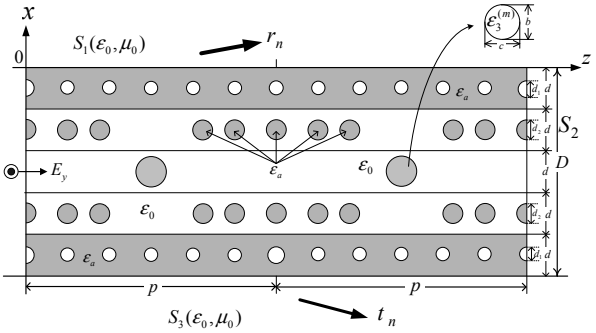

Fig.1 Coordinate system and structure of dielectric waveguide Composed of dielectric circular cylinder array with air-hole

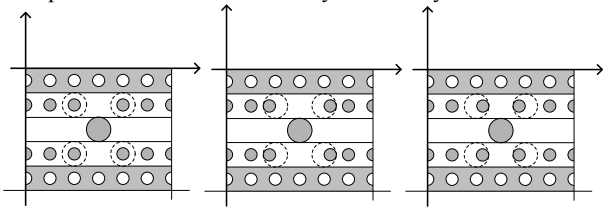

(a)Type I (b)Type II (c)Type III

Fig.2 Structures of dielectric waveguide analysis

The electromagnetic fields of all regions to satisfy the Maxwell equations are expressed as follows: [3-4]

$$E_y^{(1)} := e^{i\gamma z}\sum_{n=-N}^{N} r_n e^{ik^{(n)}x+i2n\pi z/p}, \quad (1)$$

$$E_y^{(2)} := \sum_{v=1}^{2N+1}[A_v^{(l)}e^{-ih_v^{(l)}\{x+(l-1)d_0\}} + B_v^{(l)}e^{ih_v^{(l)}\{x+ld_0\}}]f_v^{(l)}(z), \quad (2)$$

$$E_y^{(3)} := e^{i\gamma z}\sum_{n=-N}^{N} t_n e^{-ik^{(n)}(x+D)+i2n\pi z/p}, \quad (3)$$

$$f_v^{(l)}(z) := e^{i\gamma z}\sum_{n=-N}^{N} u_{v,n}^{(l)} e^{i2n\pi z/p}, \ (1 \le l \le M) \quad (4)$$

$$H_x^{(j)} := \frac{-1}{i\omega\mu_0}\frac{\partial E_y^{(j)}}{\partial z}, \ H_z^{(j)} := \frac{1}{i\omega\mu_0}\frac{\partial E_y^{(j)}}{\partial x}, \quad (5)$$

where,

$$k^{(n)} := \sqrt{k_0^2 - (\gamma + 2n\pi/p)^2}, \ d_0 := d/M, \ k_0 := 2\pi/\lambda,$$

$k^{(n)}$ and $\gamma(:=\beta+i\alpha)$ is propagation constants in the x and z-directions, respectively. k_0 is the wavenumber in free space and M is the multilayer division number. And also $A_v^{(l)}, B_v^{(l)}, r_n, t_n$ are unknown coefficients to be determined from boundary conditions. Using the boundary conditions at $x = 0, -ld_0, -D$, we obtain the following matrix equation in regard to $\mathbf{A}^{(3M)}$ at the middle layer($-3d < x < -2d$),

$$\mathbf{W}\cdot\mathbf{A}^{(3M)} = 0 \ (\det(\mathbf{W}) = 0), \quad (6)$$

In order to analyze the energy distribution, we employ the Poynting vector. The calculation of energy distribution are given by [3-4]

$$P^{(TE)} := \sqrt{\{S_x^{(TE)}\}^2 + \{S_z^{(TE)}\}^2}, \quad (7)$$

3. Numerical analysis

In the following analysis, we use the parameters $D/p = 5/6$, $\varepsilon_a/\varepsilon_0 = 3$, $\varepsilon_1/\varepsilon_0 = 3$, $d_1/d = d_2/d = 0.5$, and show the structure of dielectric waveguide as shown in Fig.2.

Figures 2(b) and (c) show the structure which slightly shifted dielectric circular cylinder near the defect region at based on type I of Fig.2(a).

Figure 3 shows the normalized frequency p/λ versus normalized attenuation constants $\alpha p/(2\pi)$ at near the first stop band region as condition of dielectric constants $\varepsilon_3^{(m)}/\varepsilon_0 = 3$ and diameter of cylinder $b/d = 1$ in the middle layer. The results of type I, II, and III are shown as black dashed line, blue dashed line, and red dashed line, respectively. And also, the black solid line is result of dielectric constants ε_0 in the middle layer. From in Fig.3, we can see the following features:

(1)We can confirm that the stop band region don't depend on the frequency for case of type I, II, and III. As reason of this result, this is because equivalent permittivity distribution in one period is same.

(2)We can see that the difference appears only maximum attenuation constants.

Figures 4(a) and (b) show comparison of the energy distribution at the guided region for types I and III as condition of same excited normalized frequency $p/\lambda = 0.4357$. From in Fig.4, we can see the following features:

(1)The energy for outside of defect area in type I are slightly smaller than those of type III.

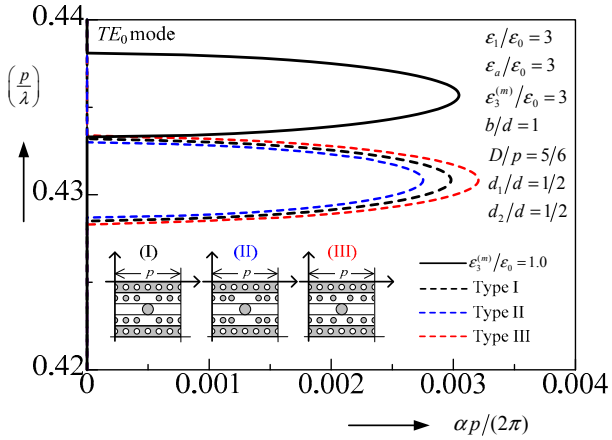

Fig.3 Normalized frequency vs. normalized attenuation constants for type I, II, and III.

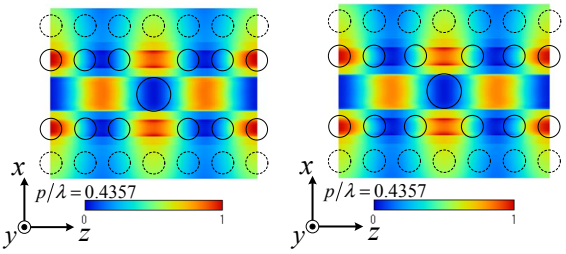

(a) Type I (b) Type III

Fig.4 Energy distribution $P^{(TE)}$ for type I and III.

(2)We can see the energy confinement of same distribution in the defect area for both types. We will have investigated the energy distribution of types I, II, and III in detail in the future.

4. Conclusion

In this paper, we analyzed the guiding problem for dielectric waveguides composed of dielectric circular cylinder array with air hole cylinder array by the case of shifting the adjacent dielectric of defect regions, and investigated the complex propagation constants at the first stop band region and energy distribution at the guiding mode.

References

[1] J. D. Joannopoulos, "Photonic Crystals, Molding the Flow of Light," *Princeton*, 2008.

[2] C. M. Soukoulis Ed., "Photonic Band Gap Materials," Kluwer Academic, 1996.

[3] R. Ozaki and T. Yamasaki, "Distribution of Energy Density by Dielectric Waveguide with Air hole Layer Composed of Dielectric Circular Cylinder Array," Proc. *URSI-GASS*, 2014, China.

[4] R. Ozaki and T. Yamasaki, "Distribution of Energy Flow by Dielectric Waveguides with Different Radius Composed of Dielectric Circular Cylinider and Air Cylinder," *Proc. ICEAA*, 2014, Aruba, pp. 97-100.